Stochastic order parameter equation of isometric force production revealed by drift-diffusion estimates

T. D. Frank,[1] R. Friedrich,[1] and P. J. Beek[2]
[1]*Institute for Theoretical Physics, University of Münster, Wilhelm-Klemm-Strasse 48149 Münster, Germany*
[2]*Faculty of Human Movement Sciences and Institute for Fundamental and Clinical Human Movement Sciences, Vrije Universiteit, Van der Boechorststraat 9, 1081 BT Amsterdam, The Netherlands*
(Received 9 March 2006; revised manuscript received 27 July 2006; published 6 November 2006)

We address two questions that are central to understanding human motor control variability: what kind of dynamical components contribute to motor control variability (i.e., deterministic and/or random ones), and how are those components structured? To this end, we derive a stochastic order parameter equation for isometric force production from experimental data using drift-diffusion estimates. We show that the force variability increases with the required force output because of a decrease of deterministic stability and an accompanying increase of noise intensity. A structural analysis reveals that the deterministic component consists of a linear control loop, while the random component involves a noise source that scales with force output. In addition, we present evidence for the existence of a subject-independent overall noise level of human isometric force production.

DOI: 10.1103/PhysRevE.74.051905 PACS number(s): 87.19.−j, 87.19.Ff, 02.50.Ey

I. INTRODUCTION

Variability is a fundamental feature of human motor control [1] and has been studied in a wide variety of contexts, including tremor [2–4], postural sway [5–12], pupil dynamics [13–15], balancing [16], stationary pointing [17], isometric force production [18,19], and coordinated movement. In the last context, variability of both discrete goal-directed movements [20] and rhythmic movements [21–29] has been examined.

In studying the emergence of motor control variability, two key issues have to be addressed. The first issue is about the nature of the dynamical processes that give rise to motor control variability. Does motor control variability originate from deterministic or random processes? In the former case, an increase of variability may be related to the decrease of the strength of a deterministic attractor. In the latter case, motor control variability scales with the amplitude of fluctuating forces. The necessity to introduce fluctuating forces into the description of a motor control system usually implies that there is another, more microscopic, level of description that is relevant besides the current level of description. The net effect of all forces originating from this more microscopic level can be regarded as a fluctuating force acting on the current level of description [30]. The second issue is a quantitative one and concerns the problem how to quantify the deterministic and random parts of motor control systems that are putatively involved in the emergence of motor control variability. Are linearized deterministic models sufficient or does the problem at hand require an account in terms of nonlinearities? Are we confronted with additive or multiplicative noise sources (probably related to power law distributions [31,32])? Several multiplicative noise motor control systems have been identified so far: the pupil dynamics [13–15], stick balancing [16], and pointing movements [17]. Moreover, arguments referring to both the structural level (e.g., motoneuron populations [33]) and the conceptual level [34] support the relevance of multiplicative noise sources for human motor control. Multiplicative noise systems are of particular interest because in this type of systems variability does not only act as a perturbing mechanism but often contributes to system functionality. For example, multiplicative noise might help to prevent neurophysiological systems from exhibiting unstable oscillations by shifting critical control parameters to higher magnitudes [15]. Multiplicative noise might also support the functioning of motor performance by stabilizing the systems on time scales shorter than reaction time scales [16]. In this context it may also be noted that variability in general might be useful for exploring task spaces and performing explorative movements [5,6] including the exploitation of stochastic resonance for the purpose of postural stabilization[12].

In the following, we will address the aforementioned issues concerning (i) the nature and (ii) the structure of the dynamical processes involved in the emergence of motor control variability. We will address these issues in the context of isometric force production. That is, we will study a force that is produced by muscles that do not change length during force production [75]. In contrast to previous studies that examined isometric force productions on a descriptive level using various kinds of descriptive measures (such as variance, correlation functions, Fourier components, statistical entropy measures [18,19]), we study isometric force production from the dynamical systems perspective of human motor control [35–39]. Accordingly, we will draw our conclusions on the basis of an order parameter equation for isometric force production. In order to derive the order parameter equation from experimental data, we will exploit drift-diffusion estimates [40,41] that have been applied to various systems including turbulence [40–42], solitons [43,44], financial systems [45,46], surface patterns [47–49], traffic flows [50], muscle tremor [4], and heart rate dynamics [51]. We will focus on the dynamics of force production close to fixed points defined by required forces. To this end, we will evaluate bulk data that is centered around mean values and constitutes approximately 98.8% of the total recorded data.

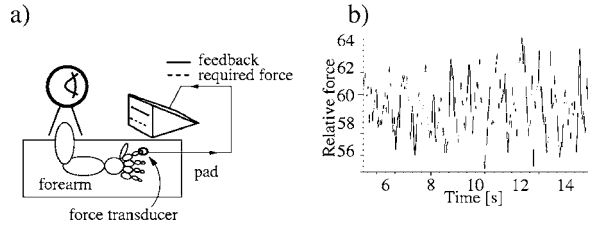

FIG. 1. Experimental setup (a) and a typical trajectory recorded during the experiment (b).

Consequently, the dynamics of rare events will not be addressed in our study. The experimental setup and the data analysis method will be explained briefly in Sec. II. We will then present our results in Sec. III.

II. EXPERIMENTAL SETUP AND DATA ANALYSIS

A. Experimental setup

Nine healthy subjects from a university population (aged 23 to 33 years, weight 69±12 kg, height 176±11 cm, two females, seven males) volunteered to participate in the experiment. All subjects described themselves as right-hand dominant. The subjects were seated in front of a computer screen with the right forearm on a pad, see Fig. 1 panel (a). They were invited to press with the fingertip of the right index finger on a Scaime force transducer (type F60X10; accuracy of 0.017%; SCAIME Inc., Annemasse Cedex, France). The output of the force transducer was amplified with a SCXI-1121 bridge amplifier and sampled continuously at a sampling rate of $f=1000$ Hz using an analog-to-digital converter (type PCI-MIO-16E-4; National Instruments, Inc., Austin, USA). For each subject the experiment consisted of two parts: assessment of the subject's maximum voluntary force $F_{\max}$ and analysis of force variability.

In order to determine the $F_{\max}$ of a subject, the subject was instructed to produce as much force as possible with his/her index finger for a duration of 10 s. The trajectory of the produced force as a function of time was displayed on the screen and the maximum value of the trajectory was determined. Three maximum values were determined by means of this procedure. The average was used as the subject's $F_{\max}$.

In order to account for the subject-dependent ability to produce muscular finger forces, produced force is usually scaled to the $F_{\max}$ values of subjects. Accordingly, in the analysis of force variability, subjects were asked to produce required forces corresponding to particular percentages of their $F_{\max}$ values. The percentages will be referred to as force levels. For example, a force level of 60 means that a subject was instructed to produce 60% of his or her maximum voluntary force over a particular period of time. In order to assist subjects in performing the task successfully, a horizontal bar on the screen (dashed line in Fig. 1) indicated the force that subjects had to produce (required force). A second horizontal bar (solid line in Fig. 1) indicated the amount of force that was actually produced by the subjects by pressing on the force transducer. Consequently, subjects had to match the feedback signal (solid line in Fig. 1) with the target line (dashed line in Fig. 1) whose height was adjusted such that it represented the required force F_{reg} ($F_{\text{reg}}=F_{\max}\times$ force level/100). Subjects had to perform five force levels L given by $L=10$, 20, 40, 60, 70 for a duration of 15 s. Each force level was tested 15 times leading to a total number of 75 trials per subject. Those 75 trials were presented in random order. In order to reduce the effect of fatigue there were five blocks of 15 trials with five minutes breaks (default value) between two blocks. Upon request subjects could prolong the break to a maximum of 15 minutes.

All experimental procedures were in accordance with the Helsinki Declaration of the World Medical Associations, and approved by the Faculty of Human Movement Sciences of the Vrije Universiteit, Amsterdam.

B. Data analysis

Data analysis was based on produced relative force defined as

$$X(t) = 100\frac{F(t)}{F_{\max}}, \tag{1}$$

where $F(t)$ denotes the produced absolute force. As mentioned earlier, the rationale for this procedure is that different subjects can be compared with each other if the performance output of a subject is scaled to his or her physical condition, that is, to the overall ability to produce isometric forces. Note that in our study, the relative force corresponds to the percentage of a subject's maximum voluntary force (e.g., 60 means a subject produces 60% of his or her $F_{\max}$), which is the reason why we have put the factor 100 into Eq. (1). In line with the dynamical systems approach to human motor control, we assumed that the evolution of $X(t)$ is determined by a stochastic order parameter equation. In the time-discrete case the order parameter equation was assumed to correspond to a time-discrete Ito Langevin equation of the form [52]

$$X(t+\Delta t) = X(t) + \Delta t h(X) + \sqrt{\Delta t D(X)}w(t) \tag{2}$$

with $t=n\Delta t$ and $n=1,\ldots,N$. For the linear case see also the alternative time-discrete representation of Eq. (2) discussed in Refs. [30,53,54]. Note that Δt corresponds to the sample interval $\Delta t=1/f$. Furthermore, $w(t)$ corresponds to a statistically-independent Gaussian distributed random variable with $\langle w\rangle=0$ and $\langle w(n\Delta t)w(n'\Delta t)\rangle=2\delta_{nn'}$, where $\delta_{nn'}$ is the Kronecker symbol. The function $h(x)$ is referred to as the drift coefficient and reflects the deterministic part of the motor control system. The function $D(x)$ will be referred to as the diffusion coefficient and describes the noise source of the system. As suggested in [40,41], the drift and diffusion functions were computed from the time-discrete data $X(t)$ using conditional averages of the form $\langle\cdots\rangle|_{X(t)=x}$. From Eq. (2) it follows that

$$h(x) = \frac{1}{\Delta t}\langle X(t+\Delta t) - X(t)\rangle|_{X(t)=x} \tag{3}$$

and

$$D(x) = \frac{1}{2\Delta t}\langle [X(t+\Delta t) - X(t) - \Delta t h(x)]^2\rangle|_{X(t)=x} \tag{4a}$$

$$\approx \frac{1}{2\Delta t}\langle [X(t+\Delta t)-X(t)]^2\rangle|_{X(t)=x}. \tag{4b}$$

Note that the approximation in Eq. (4b) becomes exact for $\Delta t \to 0$ [52]. In order to avoid concerns about the applicability of the approximation to our data set, $D(x)$ was estimated on the basis of Eq. (4a). In line with thermodynamical approaches to nonequilibrium systems [55], we assumed that $D(x)$ is a product of a parameter Q and a mobility function $M(x)$: $D(x)=QM(x)$. The parameter Q is usually referred to as noise amplitude and is often regarded as the counterpart of the temperature of equilibrium systems. Both in equilibrium and in nonequilibrium systems the mobility coefficient relates generalized thermodynamic fluxes to generalized thermodynamic forces [55]. In our context, by decomposing D into two factors Q and M we accounted for the working hypothesis that noise amplitudes may differ considerably between subjects but relative changes of noise amplitudes due to change in force requirements should be consistent across subjects. In line with this working hypothesis, the noise amplitude Q was regarded as a subject-dependent scaling factor just as the maximum voluntary force $F_{\max}$. Since Q was regarded as a scaling parameter and was by definition invariant to force requirement [see also Eq. (6) below], the mobility parameter M was used to study the impact of force requirement on isometric force production. In what follows, we will refer to Q as the mean noise level of a subject.

In order to compute $h(x)$, Q and $M(x)$ from $X(t)$, only the last ten seconds of a trial were evaluated [i.e., $X(t)$ for $t \in [5s, 15s]$]. In doing so, data analysis was based on the stationary performance and the transient ramp-up phase of force built up was discarded. Ensemble averages occurring in Eqs. (3) and (4) were then replaced by time averages.

Due to the finite length of our data sets (i.e., $n=1,\ldots,N$), the functions $h(x)$ and $M(x)$ were estimated in two steps [40,43]. In the first step, averages of $h(x)$ and $M(x)$ over particular intervals $I_i=[a_i,b_i]$ were obtained. They will be denoted by $h[i]$ and $M[i]$, respectively. In the second step, statistical analysis and interpolation techniques were used to estimate $h(x)$ and $M(x)$ on the basis of $h[i]$ and $M[i]$.

One crucial issue should be pointed out. In order to apply statistical inference analysis across individual subjects, the length of the intervals I_i was adjusted to the force variability of subjects. The interval length was chosen as one standard deviation of $X(t)$ as found for a particular subject and force level. Five such intervals (segments) were used: $I_1=[-2.5\sigma,-1.5\sigma]$, $I_2=[-1.5\sigma,-0.5\sigma]$, $I_3=[-0.5\sigma,0.5\sigma]$, $I_4=[0.5\sigma,1.5\sigma]$, $I_5=[1.5\sigma,2.5\sigma]$. Consequently, the drift segments $h[i]$ were computed from

$$h[i]=\frac{1}{\sigma}\int_{I_i} h(x)dx. \tag{5}$$

The mean noise level Q of a given subject was computed from

$$Q=\frac{1}{25\sigma}\sum_{\mathrm{FL}}\int_{-2.5\sigma}^{2.5\sigma} D(x)dx. \tag{6}$$

As can be seen from Eq. (5), the parameter Q corresponds to the average over diffusion coefficients computed from all five segments I_i and all five force levels $L=10$, 20, 40, 60, 70. Once the parameter Q was determined, the mobility segments $M[i]$ were computed from

$$M[i]=\frac{1}{\sigma Q}\int_{I_i} D(x)dx. \tag{7}$$

From the definition of the intervals I_i it follows that $h[i]$, Q and $M[i]$ were computed on the basis of approximately 98.8% of the total recorded data. The remaining recorded data that represents rare events of extremely low or high forces was not used for the derivation of $h[i]$, Q, and $M[i]$.

Statistical hypothesis testing ($\alpha=0.05$) was carried out on the subject population. Results were considered as statistically significant if there was a probability of less then 5% of a type I error ($p<0.05$).

III. RESULTS

A. Performance

Figure 1 [panel (b)] provides an example of a time series obtained in the experiment. In Fig. 1 the relative force produced by an individual subject is shown as a function of time for a typical trial. In this example, the force level was 60. Clearly visible are the two main properties of the time series. On the one hand, the time series has a mean close to the required force level. On the other hand, it exhibits fluctuations. All subjects except subject 8 performed the task successfully in all conditions. Subject 8 failed to sustain the required force at force levels 60 and 70 (i.e., there were repeated force breakdowns down to forces of zero Newton). Therefore, for subject 8 all data concerning the force levels 60 and 70 were excluded from further analysis.

As shown in Fig. 2 the produced mean force of the population increased with required force level. This increase was significant [$F(4,38)=60.2$, $p<0.05$]. Likewise, the mean variance of the population increased with the force requirement, see Fig. 3. Also this increase was significant [$F(4,38)=19.0$, $p<0.05$].

B. Deterministic part

Figure 4 shows the drift segments $h[i]$ obtained for the force level 40 averaged over the subject population. We found that the segments $h[i]$ decreased monotonically from positive to negative values. For all other force levels qualitatively similar results were obtained. The decrease of $h[i]$ as a function of i shown in Fig. 4 for the force requirement of 40 was statistically significant [$F(4,40)=7.3$, $p<0.05$]. In fact, for all other force levels the decrease of $h[i]$ was found to be significant as well [$L=10$: $F(4,40)=6.4$, $p<0.05$; $L=20$: $F(4,40)=5.8$, $p<0.05$; $L=60$: $F(4,35)=3.9$, $p<0.05$; $L=70$: $F(4,35)=3.2$, $p<0.05$]. In view of the monotonic de-

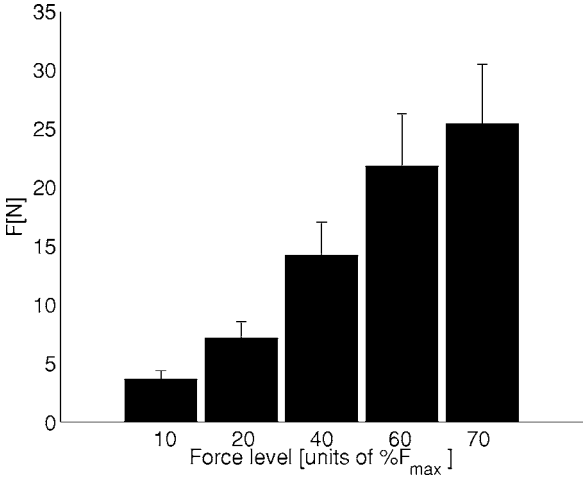

FIG. 2. Mean produced force F as a function of force level (population averages). Here and in subsequent figures error bars correspond to one standard deviation.

crease of $h[i]$, we assumed that $h(x)$ has the form

$$h(x) = -\gamma(x - x_{\text{reg}}), \tag{8}$$

where x_{reg} denotes the required force level (i.e., we have $x_{\text{reg}}=L$). Consequently, we computed the slope or Lyapunov exponent γ from the segments $h[i]$ using regression analysis. The γ parameters for individual subjects and force levels are given in Table I. The mean Lyapunov exponent (population average) as a function of the force level is shown in Fig. 5. As illustrated in Fig. 5, on average γ decreased as a function of force requirement ($\gamma_{10} > \gamma_{20} > \gamma_{40} > \gamma_{60} > \gamma_{70}$). This significant decrease $[F(4,38)=19.2, p<0.05]$ of γ was analyzed further using t tests (one-tailed; LSD design) between consecutive force levels. Significant decreases were found between the force levels 10 and 20 $[t(38)=4.3, p<0.05]$ and the force levels 20 and 40 $[t(38)=2.4, p<0.05]$. The decrease in γ from 40 to 60 was not significant, nor was the decrease in γ from 60 to 70.

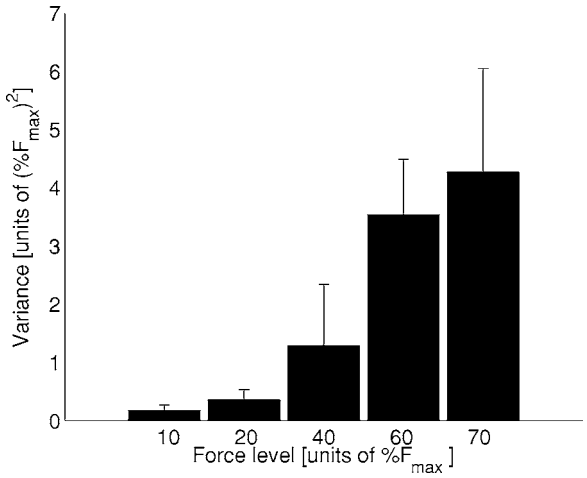

FIG. 3. Mean variance of the relative force X as a function of force level (population averages).

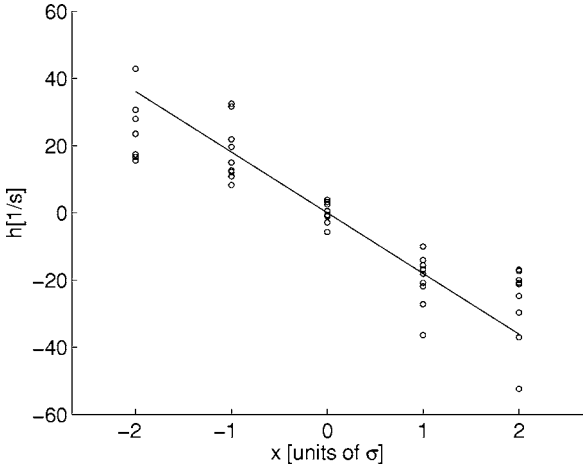

FIG. 4. Ordinate: drift segments $h[i]=\sigma^{-1}\int_{I_i} h(x)\,dx$ for force level 40 (subject-individual 15-trial averages). Abscissa: centers of segment intervals I_i $(i=1,2,3,4,5)$ at $x=\{-2\sigma,-\sigma,0,\sigma,2\sigma\}$. The slope of the regression line equals the γ coefficient shown in Fig. 5.

C. Noise

The mean noise levels Q computed from Eq. (6) for the subjects that participated in our experiment are shown in Fig. 6. Figure 6 also shows the maximum voluntary force (F_{max}) values and, consequently, illustrates the two fundamental subject-dependent parameters discussed so far. However, as we will show in Sec. III E the two parameters F_{max} and Q were correlated.

Figure 7 depicts the mean segments $M[i]$ (population averages) obtained for force level 40 as computed from Eq. (7). The small variations shown in Fig. 7 were not significant. Qualitatively similar figures were obtained for all other force levels. Again, for all other force levels variations between segments $M[i]$ were not statistically significant. Consequently, for each force level $M(x)$ could be approximated by a constant mobility coefficient M given by the average $M=\Sigma_i M[i]/5$. The M values for all subjects and force levels are reported in Table I. As shown in Fig. 8, we found that the mobility parameters depended on the force level. Figure 8 depicts population averages of the M parameters for all force requirements. The population averages increased with force ($M_{10}<M_{20}<M_{40}<M_{60}<M_{70}$). The increase was significant $[F(4,38)=23.4, p<0.05]$. t tests (one-tailed; LSD design) between consecutive force levels showed that increases between 10 and 20 % force requirements $[t(38)=1.7, p \approx 0.05]$ and between 20 and 40 % force requirements $[t(38)=1.7, p\approx 0.05]$ were significant. In contrast, increases between 40% and 60% force requirements and between 60 and 70% force requirements were not significant. In sum, the diffusion coefficient $D(x)$ was found to be of the form

$$D(x) = QM. \tag{9}$$

Equation (9) states that for each force level the diffusion coefficient $D(x)$ is the product of an overall noise level Q, which is independent of the force requirement, and a mean mobility parameter M, which increases as a function of the force requirement.

TABLE I. Lyapunov exponents γ and dimensionless mobility coefficients M for individual subjects and force levels

Subject	$\gamma[1/s]$					M				
	10	20	40	60	70	10	20	40	60	70
1	144.6	49.6	11.1	6.3	7.1	0.88	0.97	1.02	1.07	1.05
	(26.5)	(5.2)	(0.8)	(0.6)	(0.7)	(0.07)	(0.02)	(0.02)	(0.07)	(0.05)
2	172.4	107.9	57.1	12.4	11.1	0.92	0.96	1.00	1.05	1.08
	(16.3)	(13.2)	(5.3)	(1.6)	(1.3)	(0.07)	(0.03)	(0.02)	(0.03)	(0.05)
3	316.5	129.3	15.0	5.5	2.9	0.86	0.92	1.01	1.12	1.09
	(14.1)	(12.7)	(2.0)	(0.3)	(0.4)	(0.06)	(0.03)	(0.04)	(0.08)	(0.06)
4	166.0	39.5	15.6	5.3	3.8	0.94	0.99	0.99	1.03	1.06
	(12.9)	(10.8)	(2.6)	(0.5)	(0.1)	(0.05)	(0.03)	(0.02)	(0.02)	(0.02)
5	79.7	47.5	25.2	6.8	7.3	0.92	0.95	0.94	1.10	1.09
	(22.4)	(10.4)	(2.4)	(0.8)	(0.6)	(0.05)	(0.04)	(0.02)	(0.17)	(0.15)
6	188.7	78.8	16.1	3.9	3.1	0.89	0.93	0.98	1.09	1.10
	(28.0)	(9.7)	(2.6)	(0.6)	(0.3)	(0.02)	(0.06)	(0.03)	(0.08)	(0.01)
7	66.1	31.2	6.8	4.3	3.4	0.88	0.95	0.97	1.09	1.13
	(9.8)	(1.9)	(0.5)	(0.3)	(0.6)	(0.01)	(0.05)	(0.02)	(0.08)	(0.12)
8	73.9	39.9	5.3			0.96	0.96	1.09		
	(10.9)	(5.7)	(0.8)			(0.06)	(0.02)	(0.18)		
9	100.7	45.2	10.3	2.4	2.2	0.84	0.88	0.88	1.07	1.32
	(9.8)	(8.3)	(1.5)	(0.1)	(0.2)	(0.02)	(0.04)	(0.02)	(0.20)	(0.54)

D. Self-consistency test

After having determined the drift and diffusion coefficients $h(x)$ and $D(x)$ of our Langevin model (2), the question arose to what extent the model reproduced the observed data. More precisely, we examined whether or not the time-continuous version of Eq. (2) was consistent with the experimental data. Applying the limiting procedure $\Delta t \to 0$ to Eq. (2) and using the explicit expressions for $h(x)$ and $D(x)$ as given by Eqs. (8) and (9), the time-continuous Langevin model for isometric force production reads

$$\frac{d}{dt}X = -\gamma[X(t) - x_{\text{reg}}] + \sqrt{QM}\Gamma(t). \tag{10}$$

Here, $\Gamma(t)$ is a Langevin force [52] with $\langle\Gamma\rangle = 0$ and $\langle\Gamma(t)\Gamma(t')\rangle = 2\delta(t-t')$, where $\delta(\cdots)$ denotes the Dirac delta function. The Langevin model (10) predicts a variance of

$$\sigma^2 = \frac{QM}{\gamma}. \tag{11}$$

The model-based variance (11) was computed from the Q values shown in Fig. 6 and the M and γ values reported in

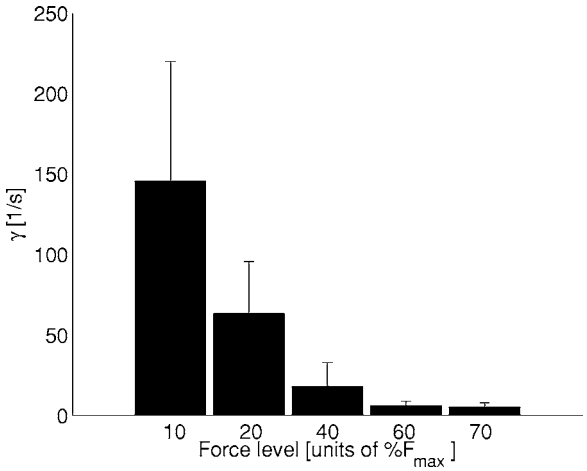

FIG. 5. Mean Lyapunov exponent γ as a function of force level (population averages).

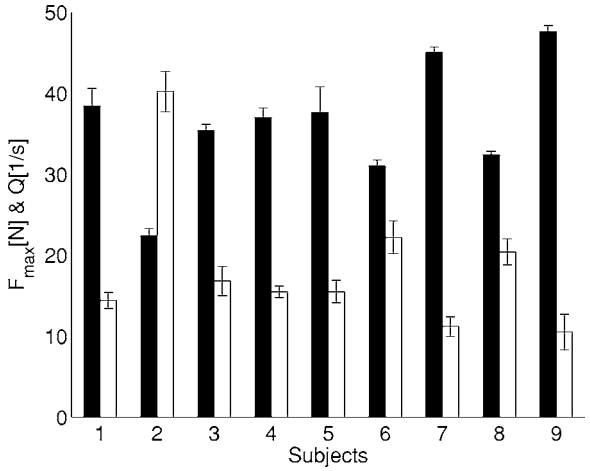

FIG. 6. Maximum voluntary force $F_{\max}$ (black bars) and mean noise level Q (white bars).

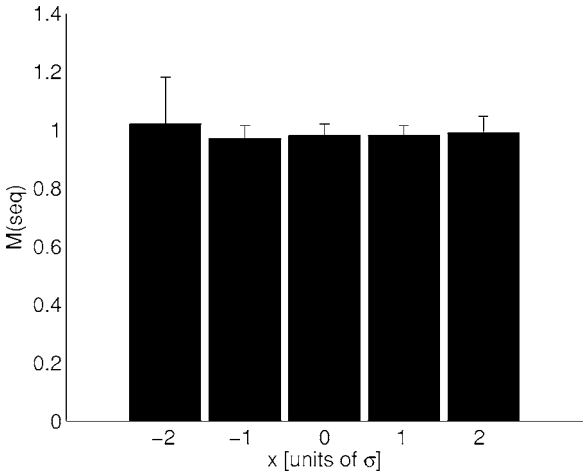

FIG. 7. Ordinate: dimensionless mobility segments $M[i]=(\sigma Q)^{-1}\int_{I_i}D(x)\,dx$ for force level 40 (population averages). Abscissa: centers of segment intervals I_i $(i=1,2,3,4,5)$ at $x=\{-2\sigma, -\sigma,0,\sigma,2\sigma\}$.

Table I. The so obtained population mean values of the σ^2 values are shown in Fig. 9 (white bars) and compared with the respective experimentally observed mean values (black bars). We found that predicted and observed variances were of the same order of magnitude. t tests showed that the predicted variances were not significantly different from the observed variances. That is, we found that the time-continuous Langevin model (10) provides a good approximative description for isometric force production.

E. Nature of the noise levels Q

In order to check whether the subject-dependent parameters $F_{\max}$ and Q were correlated, we rearranged the subjects on the horizontal axis of Fig. 6 according to their $F_{\max}$ values. The result is shown in Fig. 10 and clearly reveals a negative correlation between $F_{\max}$ and Q. In fact, we found a correlation coefficient ρ of $\rho=-0.94$. In order to explain this correlation, we hypothesized that the mean noise level did

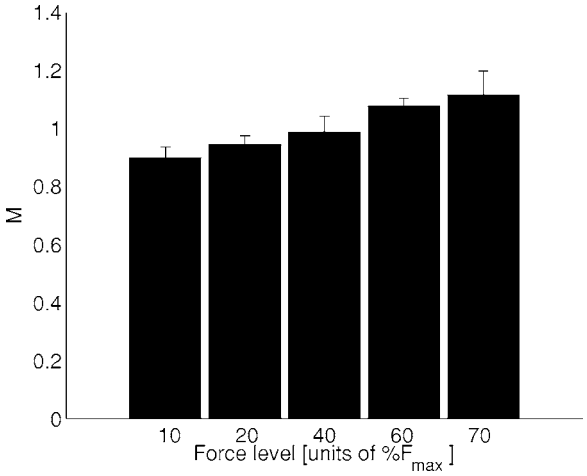

FIG. 8. Dimensionless mean mobility coefficient M as a function of force level (population averages).

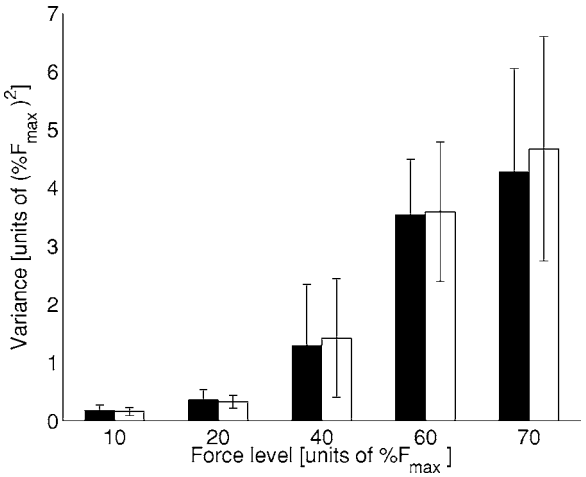

FIG. 9. Mean variance as a function of force level (population averages). Experimental results (black bars) versus predictions made by the Langevin model (10) (white bars).

not scale with the maximum voluntary force. Accordingly, the mean noise level had to be computed directly from the produced forces $F(t)$ and not from the relative forces $X(t)$ [see also Eq. (1)]. If this hypothesis would be correct, we would get $q=F_{\max}^2 Q$. If q reflects a subject-independent constant, then Q and $F_{\max}$ must be negatively correlated. To test the hypothesis, we computed q from

$$q=\frac{1}{25\sigma}\sum_{\mathrm{FL}}\int_{-2.5\sigma}^{2.5\sigma}D(F)dF, \tag{12}$$

just as we did for Q [see Eq. (6)]. Figure 11 depicts the obtained q values. All q values were centered around a population mean value of $\bar{q}=22000(\pm 1000)\ \mathrm{N}^2/\mathrm{s}$. There was a weak tendency for q to decrease with decreasing $F_{\max}$ (we found $\Delta q=q/\bar{q}\propto 0.007F_{\max}$; compare also Figs. 10 and 11). However, this tendency and the differences between q-parameters were not statistically significant. This result

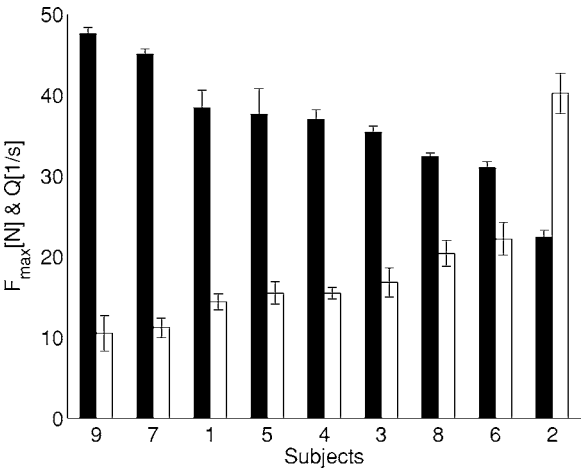

FIG. 10. Subject parameters $F_{\max}$ (black bars) and Q (white bars) as in Fig. 6 but with subjects sorted according to decreasing parameters $F_{\max}$.

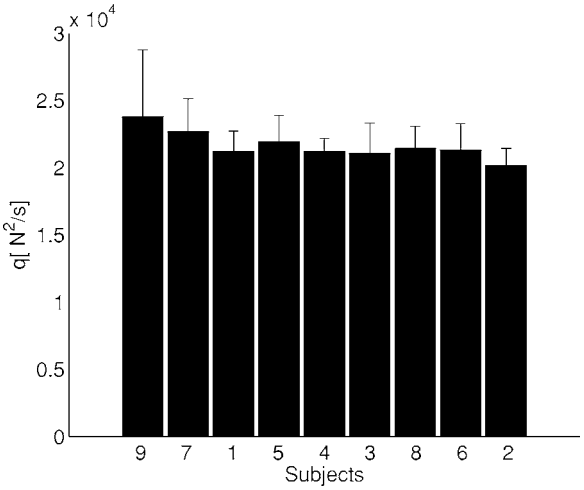

FIG. 11. Mean noise level q as computed from Eq. (12) for individual subjects.

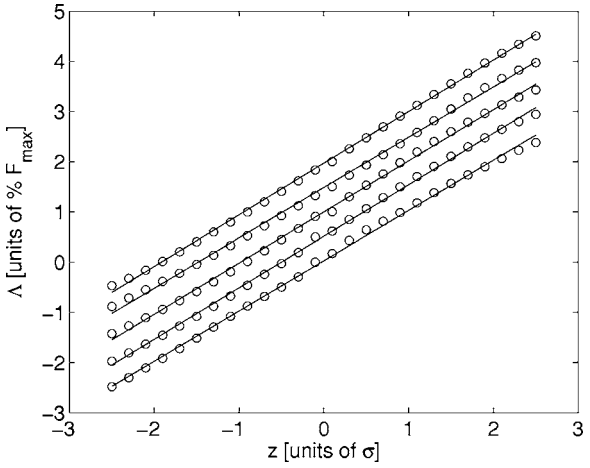

FIG. 12. Circles: $\Lambda(z)=\sqrt{-2\ln[P(z)/P_{\max}]}$ versus z of the rescaled force distribution $P(z)$ (with vanishing mean and variance equal to 1) for several force levels L. Solid lines: regression lines. Gaussian distributions would satisfy $\Lambda(z)=\beta z$ with $\beta=1$. From bottom to top: $L=10$, 20, 40, 60, 70. Graphs are shifted by 0.5 along the y axis for the sake of clarity. Slope parameters β and 95% confidence intervals $\beta_{10}=1.00$ [0.98, 1.02], $\beta_{20}=1.03$ [1.01, 1.04], $\beta_{40}=1.02$ [1.00, 1.04], $\beta_{60}=1.00$ [0.98, 1.02], $\beta_{70}=1.03$ [1.02, 1.04]. All R^2 values were larger than 0.99. Rescaled force distributions $P(z)$ were computed using the MATLAB probability density estimator.

supported our hypothesis of a subject-independent noise level that did not scale with $F_{\max}$ values.

Note that expressing the noise level in terms of Q or q is just a matter of choosing different units. Therefore, all previous arguments given in Secs. III C and III D concerning the mobility coefficient M and the appropriateness of the time-continuous Langevin model would remain valid if we would replace Q by $q/(F_{\max})^2$. In other words, the analyses in the previous sections in combination with the finding of a subject-independent constant q suggested that the Langevin equation of isometric force production should read

$$\frac{d}{dt}X = -\gamma[X(t)-x_{\text{reg}}]+\frac{1}{F_{\max}}\sqrt{qM}\Gamma(t), \tag{13}$$

where q is a parameter that did not change significantly across subjects.

F. Model plausibility and generalizations

For a given force requirement the Langevin model (10) describes an Ornstein-Uhlenbeck process [52]. We would like to discuss now under which conditions it is also plausible to assume that isometric force production is described by an Ornstein-Uhlenbeck process and how the model should be generalized if these conditions are violated.

1. Multiplicative noise and power laws

First of all, the Ornstein-Uhlenbeck model predicts that produced forces abide a Gaussian distribution. In order to check this prediction, we transformed produced relative forces X into random variables with vanishing mean and unit variance as follows: $X\rightarrow z=(X-\langle X\rangle)/\sigma$. We checked whether the respective rescaled probability densities $P(z)$ involved the characteristic parabolic potentials z^2 of Gaussian (i.e., normal) distributions. To this end, we plotted the quantity $\Lambda(z)=\sqrt{-2\ln[P(z)/P_{\max}]}$ with $P_{\max}=P(0)$ versus z. For Gaussian distributions there would be a linear relationship $\Lambda\propto z$. For the forces considered in our study (force range defined by 2.5 standard deviations around required forces) the empirical distributions $P(z)$ clearly exhibited such a linear relationship $\Lambda\propto z$, see Fig. 12 (all R^2 values of linear regression analysis were larger than 0.99).

In general, we would expect to observe non-Gaussian distributions (e.g., power-law distributions [31,32]) related to nonlinear drift terms $h(x)$ and multiplicative noise terms $D(x)$. Nonlinear drift terms would reveal more specific details of the deterministic processes involved in isometric force production. Multiplicative noise would reveal the impacts of fluctuating parameters and fluctuating external driving forces. In order to uncover non-Gaussian distributions with power-law tails and other kinds of non-Gaussian tails from experimental data a statistics appropriate for rare events is needed. Our experimental design was tailored to investigate the statistics and stochastic dynamics of isometric force production close to fixed points defined by required forces. Around these fixed points, however, potential impacts of nonlinearities and multiplicative noise terms should become small. Therefore, it is plausible to assume that a linear drift model with an additive noise term provides an appropriate description—an assumption that is in line with our experimental findings. Changing the experimental protocol in order to study isometrically produced force that exhibits more unlikely events would probably require to generalize the Ornstein-Uhlenbeck model (10) to incorporate nonlinear drifts and multiplicative noise terms, see Table II.

2. Time delays

The Langevin model (10) does not account for time-delayed neurophysiological feedback loops. Such feedback

TABLE II. Generalizations and rescaling techniques related to the Ornstein-Uhlenbeck model (10)

Generalizations		Rescaling	
Nonlinear drift	Multiplicative noise	Time delay τ	Noise correlation time τ
$-\gamma x \rightarrow h(x)$	$M \rightarrow M(X)$	$\gamma_d = \gamma(1+\gamma\tau)$	$\gamma_c = \gamma$
		$Q_d = Q$	$Q_c = \frac{\tau}{\Delta t} Q$

loops can be modeled by means of time-delayed Langevin equations [9,15,16]. Time-delayed feedback crucially determines the transient dynamics of a system. In the stationary linear case, however, we can deal with feedback loops involving small neurophysiological time delays τ by rescaling the model parameters of nondelayed models. For example, the time-delayed generalization of Eq. (10) given by $dX/dt = -\gamma_d[X(t-\tau)-x_{\mathrm{reg}}] + \sqrt{Q_d M}\Gamma(t)$ can be mapped to Eq. (10) by putting $\gamma_d = \gamma(1+\gamma\tau)$ [56,57]. Moreover, as shown in Ref. [57] for arbitrary time delays τ we have $Q_d = Q$, see also Fig. 13. In sum, we see that due to this rescaling procedure the Lyapunov exponent γ_d of the time-delayed model for isometric force production is smaller than the respective parameter of the Ornstein-Uhlenbeck model (10), while the diffusion coefficient is not affected by the length of the time delay, see Table II.

In order to study in more detail the impacts of time delays on isometric force production, the experimental design described in Sec. II A could be modified and the time delay of the visual feedback loop could be manipulated experimentally [17,58,59]. In particular, in such experimental studies isometric force production under the impact of relatively large time delays could be examined. In this case, however, the Langevin model (10) should be replaced by the aforementioned time-delayed version because for large time delays the rescaling approach listed in Table II for the Lyapunov exponent γ fails.

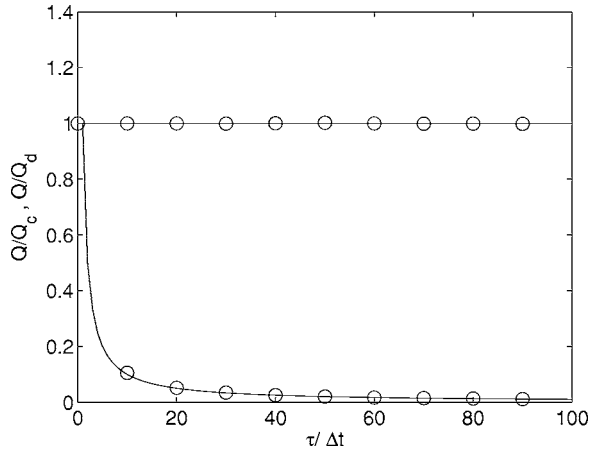

FIG. 13. Q/Q_d (top graph) and Q/Q_c (bottom graph) as functions of the relative time delay and the relative correlation time $\tau/\Delta t$, respectively. Both theoretical (solid lines) and numerical (circles) results are shown. Top: $Q/Q_d = 1$ (theory); $dX/dt = -\gamma_d[X(t-\tau)-x_{\mathrm{reg}}] + \sqrt{Q_d M}\Gamma(t)$ (numerical model). Bottom: $Q/Q_d = \Delta t/\tau$ (theory) and $dX/dt = -\gamma_c[X(t)-x_{\mathrm{reg}}] + \sqrt{Q_c M}\zeta(t)$ with $d\zeta(t)/dt = -\tau^{-1}[\zeta(t) - \sqrt{2}\Gamma(t)]$ (numerical model). Other simulation parameters (top and bottom): $x_{\mathrm{reg}} = 0$, $\gamma_d = \gamma_c = M = 1$. Ratios Q/Q_d, Q/Q_c, $\tau/\Delta t$ are shown as dimensionless quantities. Numerics as in Ref. [52].

3. Colored noise

The Langevin approach centered around Eq. (10) involves a δ-correlated fluctuating force. δ-correlated fluctuating forces are useful approximations of fluctuating forces involving short but finite correlation times (colored noise) [60]. In some examples, however, it has been argued that human motor control systems are driven by colored rather than δ-correlated noise [9,15]. Although the Ornstein-Uhlenbeck model (10) involves δ-correlated noise, it can account to a certain extent for colored noise. As shown in Refs. [61–63], colored noise models involving short correlation times can be approximated by means of effective Langevin equations (and Fokker-Planck equations) involving δ-correlated fluctuating forces. Such an approach also holds for the data analysis method discussed in Sec. II B. For example, let us consider the linear colored noise model $dX/dt = -\gamma_c[X(t)-x_{\mathrm{reg}}] + \sqrt{Q_c M}\zeta(t)$ involving a fluctuating force $\zeta(t)$ with correlation time τ [76]. In this case a detailed calculation shows that the parameters γ_c and $Q_c$can be obtained by rescaling the parameters γ and Q occurring in the Ornstein-Uhlenbeck model (10) such as $\gamma_c = \gamma$ [64] and $Q_c = \tau Q/\Delta t$, see Fig. 13 and Table II. That is, in the presence of colored noise the actual overall noise amplitude of the motor control system is larger than estimated on the basis of the Ornstein-Uhlenbeck model (10). However, the Lyapunov exponent is not affected by the correlation time of the fluctuating force.

4. Qualitative impacts of time delays and noise correlation times

As indicated in Table II, possible impacts of (short) time delays and colored noise sources will result in quantitative changes but not in qualitative changes provided that time delays and noise correlation times do not depend on the required force. For example, the overall noise amplitudes Q_d and Q_c will behave qualitatively like the overall noise amplitude Q of the Ornstein-Uhlenbeck model (10). That is, they will not depend on the required force.

5. Plausibility of the Ornstein-Uhlenbeck model (10)

In closing these considerations, we conclude that the Ornstein-Uhlenbeck model (10) is a plausible stochastic model provided that isometric force is produced close to a required force and that time delays and noise correlation times can be neglected. In addition, (short) neurophysiological time delays and noise correlation times can be addressed by means of the Ornstein-Uhlenbeck model (10) using parameter rescaling techniques. The model (10) probably needs to be generalized if unlikely events and large time delays

(e.g., externally imposed delay times) play important roles. It also needs to be revised if the explicit objective is to examine to which extent colored noise sources are involved in isometric force production.

IV. CONCLUSIONS

We derived a stochastic order parameter equation for the relative force $X(t)$ produced in an isometric force production task. To this end, we modified a drift-diffusion estimation technique proposed earlier [40,41] such that standard statistical inference techniques could be readily applied in the data analysis. From the obtained order parameter equation we could draw several conclusions.

We found that force variability in isometric force production can be explained by a time-continuous Ito-Langevin equation. We found that both drift and diffusion coefficients of the Langevin model depended on the averaged produced force. Since the drift coefficient reflects deterministic processes and the diffusion coefficient reflects random processes, we conclude that force variability is the result of both deterministic and random processes.

In addition, we identified the structure of the deterministic and random components leading to force variability. The deterministic part can be modeled as a linear control loop, whereas the random part corresponds to a noise source that is additive (i.e., unstructured) for every force level. In other words, for a fixed force requirement the structure of the Langevin model describes an Ornstein-Uhlenbeck process [52]. As a result, for a fixed force requirement human isometric force production satisfies an optimization principle [55]. It minimizes the free energy F_E given by the functional

$$F_E = \frac{\gamma}{2}\langle (X - x_{\mathrm{req}})^2 \rangle - QMS, \tag{14}$$

where S is the Boltzmann-Gibbs-Shannon entropy [$S=-\int P \ln P \mathrm{d}x$ with $P(x)$ the stationary distribution of the Ornstein-Uhlenbeck process] and the expression $U=0.5\gamma\langle (X-x_{\mathrm{req}})^2\rangle$ can be regarded as a generalized internal energy of the human motor control system. That is, our model links the dynamical systems approach of motor control [35–39] to the optimization theory of motor control [65,66]. To illustrate this property, we computed the pseudothermodynamic variables U and F and the entropy term QMS from the γ values reported in Table I and the experimentally observed variances σ^2. According to the Ornstein-Uhlenbeck model (10), the respective expressions are given by

$$U = \frac{\gamma}{2}\sigma^2,$$

$$QMS = \frac{QM}{2}\{\ln[2\pi\sigma^2] + 1\},$$

$$F_E = \frac{\gamma}{2}\sigma^2 - \frac{QM}{2}\{\ln[2\pi\sigma^2] + 1\}. \tag{15}$$

The results are shown in Fig. 14. The internal energy did not vary much with the force level. In contrast, the entropy contribution increased, whereas the free energy decreased with required force. Obviously, the decrease of the free energy is due to the increase of the entropy contribution.

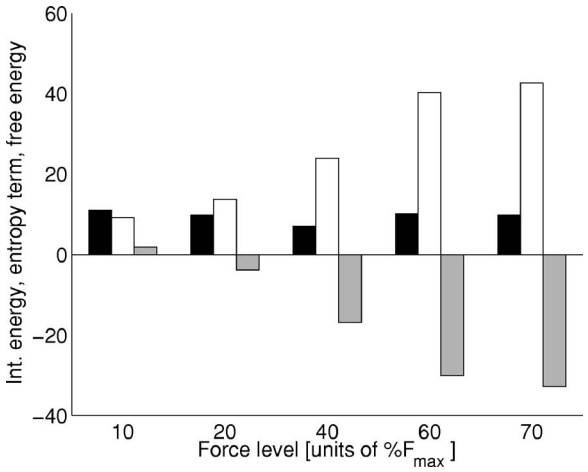

FIG. 14. Pseudothermodynamic variables (population averages) for different force levels as computed from Eq. (15): internal energy U (black), entropy term QMS (white), and free energy F_E (grey). Note that we have $F_E=U-QMS$.

We found that the noise amplitude of the random part increased as a function of the required force. That is, the noise amplitude significantly depended on the motor performance and was a function of the mean force output. A structural interpretation of this noise increase can be given in terms of the size principle of human force production [67–69]. Accordingly, if the amount of force produced by a muscle increases, then both the number of activated motor units and the averaged size of the activated motor units increases. If every single motor unit involves a particular finite amount of noise, then the overall noise will increase with the required force [77]. As mentioned in the Introduction, there are various other motor control systems that have been identified recently as multiplicative noise systems. In these studies noise amplitudes were found that depend on the state variables of the respective systems. It is important to realize that in our study the noise amplitude $D=QM$ did not depend on the state variable X but on x_{reg}. That is, according to our analysis isometric force production involves for any fixed force level x_{reg} an additive noise force (see also Sec. III F). Changes of the control parameter, that is, the force level x_{reg}, however, induced changes of the noise amplitude.

As discussed in Sec. III E, a more detailed analysis of our experimental data revealed that the overall noise levels of our subjects did not scale with the maximum voluntary forces produced by the subjects. In general, it is reasonable to assume that force variability will depend both on the physical condition of a subject and on the magnitude of the actually produced force. In contrast, our data clearly showed that in the case of isometric force production the physical condition as indexed by the maximum voluntary force was irrelevant (there was a subject-independent parameter q), whereas the required force output was a relevant quantity (the mobility M increased as a function of required force). In view of a subject-independent overall noise level q, which is related to the absolute force $F(t)$ but not to the relative force

$X(t)$, one may argue that the order parameter equation of isometric force production should be written in terms of $F(t)$ rather than in terms of $X(t)$. Using Eq. (1), we can write Eq. (13) as

$$\frac{d}{dt}F = -\gamma[F(t) - F_{\text{req}}] + \sqrt{q^* M}\Gamma(t), \tag{16}$$

where F_{req} is the required absolute force (see Sec. II A). Here q^* is given by $q^* = q/10^4$ because of the scaling factor in Eq. (1). Since q is in the order of 2×10^4 N^2/s (see Sec. III E), we see that q^* is in the order of 2 N^2/s. One may pose the question which of the two order parameter equations [Eq. (13) or (16)] is the relevant order parameter equation for isometric force production. Future experimental and theoretical studies may elucidate this point. For the time being, we just would like to point out that several previous studies on isometric force production were entirely based on the analysis of relative forces $X(t)$. That is, in those studies it was tacitly assumed that both deterministic and random components of isometric force production scale with F_{max} values. The present findings suggest that the results in those studies should be interpreted with caution.

Returning to our very first remark in this section, we demonstrated in the present study that stochastic order parameter equations of human motor control systems can be derived using drift-diffusion estimates in such a way that quantitative statements can be made and corresponding hypotheses can be tested statistically. Several studies recently showed at least qualitatively that the drift-diffusion estimation technique can be generalized to account for higher-dimensional oscillatory motor control systems [4], time delays [70–72], couplings between microsystems giving rise to macroscopic order parameter dynamics [55,73], and microsystem couplings involving time delays [74]. Since time delays as well as microsystem couplings (e.g., couplings between neural units or motor units or cross-bridge couplings in muscles) are likely to play crucial roles in human motor control, future efforts may be devoted to generalizing the theoretical and empirical results of the present study. In such efforts generalized models for isometric force production as discussed in Sec. III F may be addressed.

[1] K. Davids, S. Bennett, and K. Newell, *Movement System Variability* (Human Kinetics, Champaign, 2006).
[2] S. Morrison and K. M. Newell, Exp. Brain Res. **110**, 455 (1996).
[3] P. Tass, M. G. Rosenblum, J. Weule, J. Kurths, A. Pikovsky, J. Volkmann, A. Schnitzler, and H. J. Freund, Phys. Rev. Lett. **81**, 3291 (1998).
[4] R. Friedrich, S. Siegert, J. Peinke, S. Lück, M. Seifert, M. Lindemann, J. Raethjen, G. Deuschl, and G. Pfister, Phys. Lett. A **271**, 217 (2000).
[5] J. J. Collins and C. J. De Luca, Exp. Brain Res. **95**, 308 (1993).
[6] J. J. Collins and C. J. De Luca, Phys. Rev. Lett. **73**, 764 (1994).
[7] M. A. Riley, S. Wong, S. Mitra, and M. T. Turvey, Exp. Brain Res. **117**, 165 (1997).
[8] K. M. Newell, S. M. Slobounov, E. S. Slobounova, and P. C. M. Molenaar, Exp. Brain Res. **113**, 158 (1997).
[9] R. J. Peterka, Biol. Cybern. **82**, 335 (2000).
[10] T. D. Frank, A. Daffertshofer, and P. J. Beek, Phys. Rev. E **63**, 011905 (2001).
[11] M. Duarte and V. M. Zatsiorsky, Phys. Lett. A **283**, 124 (2001).
[12] A. Priplata, J. Niemi, M. Salen, J. Harry, L. A. Lipsitz, and J. J. Collins, Phys. Rev. Lett. **89**, 238101 (2002).
[13] L. Stark, F. W. Campbell, and J. Atwood, Nature (London) **182**, 857 (1958).
[14] S. Usui and L. Stark, Biol. Cybern. **45**, 13 (1982).
[15] A. Longtin, J. G. Milton, J. E. Bos, and M. C. Mackey, Phys. Rev. A **41**, 6992 (1990).
[16] J. L. Cabrera and J. G. Milton, Phys. Rev. Lett. **89**, 158702 (2002).
[17] K. Vasilakov and A. Beuter, J. Theor. Biol. **165**, 389 (1993).
[18] S. Morrison and K. M. Newell, J. Motor Behav. **30**, 323 (1998).
[19] A. B. Slifkin and K. M. Newell, J. Exp. Psychol. Hum. Percept. Perform. **25**, 837 (1999).
[20] P. M. Fitts, J. Exp. Psychol. **47**, 381 (1954).
[21] G. S. Schöner, H. Haken, and J. A. S. Kelso, Biol. Cybern. **53**, 247 (1986).
[22] J. P. Scholz, J. A. S. Kelso, and G. S. Schöner, Phys. Lett. A **123**, 390 (1987).
[23] C. E. Peper, P. J. Beek, and P. C. W. van Wieringen, J. Exp. Psychol. Hum. Percept. Perform. **21**, 1117 (1995).
[24] E. L. Amazeen, P. G. Amazeen, P. J. Treffner, and M. T. Turvey, J. Exp. Psychol. Hum. Percept. Perform. **23**, 1552 (1997).
[25] Y. Chen, M. Ding, and J. A. Scott Kelso, Phys. Rev. Lett. **79**, 4501 (1997).
[26] A. Daffertshofer, C. van den Berg, and P. J. Beek, Physica D **132**, 243 (1999).
[27] D. Sternad, W. J. Dean, and K. M. Newell, J. Motor Behav. **32**, 249 (2000).
[28] A. A. Post, C. E. Peper, A. Daffertshofer, and P. J. Beek, Biol. Cybern. **83**, 443 (2000).
[29] G. Madison, J. Exp. Psychol. Hum. Percept. Perform. **27**, 411 (2001).
[30] H. Haken, *Synergetics: Introduction and Advanced Topics* (Springer, Berlin, 2004).
[31] W. Horsthemke and R. Lefever, *Noise-induced Transitions* (Springer, Berlin, 1984).
[32] T. S. Biro and A. Jakovac, Phys. Rev. Lett. **94**, 132302 (2005).
[33] P. B. Matthews, J. Physiol. (London) **492**, 597 (1996).
[34] C. M. Harris and D. M. Wolpert, Nature (London) **394**, 780 (1998).

[35] M. T. Turvey, Am. Psychol. **45**, 938 (1990).
[36] P. J. Beek, C. E. Peper, and D. F. Stegeman, Hum. Mov. Sci. **14**, 573 (1995).
[37] J. A. S. Kelso, *Dynamic Patterns—The Self-organization of Brain and Behavior* (MIT Press, Cambridge, 1995).
[38] H. Haken, *Principles of Brain Functioning* (Springer, Berlin, 1996).
[39] D. Corbetta and B. Vereijken, Int. J. Sport Psychol. **30**, 507 (1999).
[40] R. Friedrich and J. Peinke, Phys. Rev. Lett. **78**, 863 (1997).
[41] R. Friedrich and J. Peinke, Photochem. Photobiol. **102**, 147 (1997).
[42] C. Renner, J. Peinke, R. Friedrich, O. Chanal, and B. Chabaud, Phys. Rev. Lett. **89**, 124502 (2002).
[43] H. U. Bödeker, M. C. Röttger, A. W. Liehr, T. D. Frank, R. Friedrich, and H. G. Purwins, Phys. Rev. E **67**, 056220 (2003).
[44] H. U. Bödeker, A. Liehr, M. C. Röttger, T. D. Frank, R. Friedrich, and H. G. Purwins, New J. Phys. **6**, 62 (2004).
[45] R. Friedrich, J. Peinke, and C. Renner, Phys. Rev. Lett. **84**, 5224 (2000).
[46] C. Renner, J. Peinke, and R. Friedrich, Physica A **298**, 499 (2001).
[47] G. R. Jafari, S. M. Fazeli, F. Ghasemi, S. M. Vaez Allaei, M. R. Tabar, A. Iraji Zad, and G. Kavei, Phys. Rev. Lett. **91**, 226101 (2002).
[48] M. Waechter, F. Riess, T. Schimmel, U. Wendt, and J. Peinke, Eur. Phys. J. B **41**, 259 (2004).
[49] P. Sangpour, G. R. Jafari, O. Akhavan, A. Z. Moshfegh, and M. R. Tabar, Phys. Rev. B **71**, 155423 (2005).
[50] S. Kriso, R. Friedrich, J. Peinke, and P. Wagner, Phys. Lett. A **299**, 287 (2002).
[51] T. Kuusela, Phys. Rev. E **69**, 031916 (2004).
[52] H. Risken, *The Fokker-Planck Equation—Methods of Solution and Applications* (Springer, Berlin, 1989).
[53] M. Kac, in *Selected Papers on Noise and Stochastic Processes*, edited by N. Wax (Dover, New York, 1947), pp. 295–317.
[54] H. Larralde, Phys. Rev. E **69**, 027102 (2004).
[55] T. D. Frank, *Nonlinear Fokker-Planck Equations: Fundamentals and Applications* (Springer, Berlin, 2005).
[56] S. Guillouzic, I. L'Heureux, and A. Longtin, Phys. Rev. E **59**, 3970 (1999).
[57] T. D. Frank, Phys. Rev. E **72**, 011112 (2005).
[58] P. Tass, J. Kurths, M. G. Rosenblum, G. Guasti, and H. Hefter, Phys. Rev. E **54**, R2224 (1996).
[59] U. Langenberg, H. Hefter, K. R. Kessler, and J. D. Crooke, Exp. Brain Res. **118**, 161 (1998).
[60] R. L. Stratonovich, *Topics in the Theory of Random Noise* (Gordon and Beach, New York, 1963), Vol. 1.
[61] J. M. Sancho, M. S. Miguel, S. L. Katz, and J. D. Gunton, Phys. Rev. A **26**, 1589 (1982).
[62] P. Hänggi, T. J. Mroczkowski, F. Moss, and P. V. E. McClintock, Phys. Rev. A **32**, 695 (1985).
[63] M. Gitterman, J. Phys. A **32**, L293 (1999).
[64] K. Patanarapeelert, T. D. Frank, R. Friedrich, P. J. Beek, and I. M. Tang (unpublished).
[65] D. F. Hoyt and C. R. Taylor, Nature (London) **292**, 239 (1981).
[66] R. M. Alexander, Physiol. Rev. **69**, 1199 (1989).
[67] E. Henneman, G. Somjen, and D. O. Carpenter, J. Physiol. (London) **28**, 560 (1965).
[68] E. Henneman, in *Integration in the Nervous System*, edited by H. Asanuma and V. J. Wilson (Igaku Shoin, Tokyo, 1979), pp. 13–25.
[69] R. A. Conwit, D. Stashuk, B. Tracy, M. McHugh, W. F. Brown, and E. J. Metter, J. Clin. Neuropsychol **110**, 1270 (1999).
[70] T. D. Frank, P. J. Beek, and R. Friedrich, Phys. Rev. E **68**, 021912 (2003).
[71] T. D. Frank, P. J. Beek, and R. Friedrich, Phys. Lett. A **328**, 219 (2004).
[72] T. D. Frank, Phys. Rev. E **69**, 061104 (2004).
[73] T. D. Frank and R. Friedrich, Physica A **347**, 65 (2005).
[74] T. D. Frank and P. Beek, J. Stat. Mech.: Theory Exp. (2005), P10010.
[75] Isometric force is also referred to as static force indicating that it does not involve a limb movement but rather holding a fixed limb position.
[76] Correlation time is defined here implicitly by means of the autocorrelation function $\langle \zeta(t)\zeta(t')\rangle = 2\tau^{-1}\exp\{-|t-t'|/\tau\}$.
[77] This argument assumes that the noise sources of the motor units are uncorrelated.